



# A FAIR comparison of activated carbon, biochar, cyclodextrins, polymers, resins, and metal organic frameworks for the adsorption of per- and polyfluorinated substances

Navid Saeidi<sup>a,b,\*</sup>, Adelene Lai<sup>c</sup>, Falk Harnisch<sup>a</sup>, Gabriel Sigmund<sup>d,\*</sup>

<sup>a</sup> Department of Microbial Biotechnology, Helmholtz Centre for Environmental Research – UFZ, 04318 Leipzig, Germany

<sup>b</sup> Department of Technical Biogeochemistry, Helmholtz Centre for Environmental Research – UFZ, 04318 Leipzig, Germany

<sup>c</sup> Water Information from Earth Observation, L-1911 Luxembourg, Luxembourg

<sup>d</sup> Environmental Technology, Wageningen University & Research, 6700 AA Wageningen, the Netherlands

## ARTICLE INFO

### Keywords:

PFAS  
Adsorbent, molecular properties  
Structure-based grouping  
Adsorption prediction  
Sorbent selection

## ABSTRACT

Per- and polyfluorinated substances (PFAS) have complex sorption behaviors, complicating removal from water and selection of suitable adsorbents. We evaluated adsorption of 44 PFAS across four adsorbent groups: activated carbon and biochar (AC and BC), cyclodextrin-based adsorbents (cyclodextrins), polymer-based adsorbents and resins, and inorganic adsorbents and metal organic frameworks (MOFs). We analyzed over 500 adsorption coefficients ( $K_d$ ) from literature, calculated at aqueous equilibrium concentration of  $1 \pm 0.3 \mu\text{g/L}$  under comparable experimental conditions. On average,  $K_d$  of AC and BC exceeded  $10^7 \text{ L/kg}$  for PFAS with C-F bonds  $> 7$ , unlike other adsorbents with  $K_d < 10^7$ . This trend holds for C-F bonds  $\geq 4$ . Cyclodextrins, polymer-based adsorbents and resins outperform AC and BC for C-F bonds  $< 4$ . For AC and BC,  $K_d$  follows the order PFOS > PFOA > PFBS > PFBA, with adsorption increasing with increasing point of zero charge of the adsorbent. For AC and BC, as well as cyclodextrins,  $K_d$  values were related to PFAS hydrophobicity and steric properties. Additionally, adsorption was influenced by head group type, non-fluorinated carbon atoms, and the presence of oxygen and/or chlorine in the PFAS. No clear relationship was found for the other adsorbents. Adsorption prediction using a Random Forest Regressor and literature data was feasible for AC and BC, but not for other adsorbents. Cyclodextrins outperform AC and BC for removing PFAS across varying mobilities from water, whereas AC and BC are superior for low mobility PFAS. To support further data use all data and code used are freely available, following FAIR data principles.

## 1. Introduction

Per- and polyfluoroalkyl substances (PFAS) constitute a diverse group of fluorinated chemicals with linear, branched and/or cyclic carbon backbones. PFAS are extremely persistent chemicals distinguished by unique physicochemical properties such as prolonged half-lives, repellence of oil and water, and thermal stability, which has led to their use in a wide range of applications [1]. The prolonged persistence, widespread utilization, and high mobility of PFAS resulted in their rapid dissemination in various sources of water, including drinking water. In the latter even very low concentrations in the ng/L to  $\mu\text{g/L}$  range are reported to threaten human health [2,3]. Thus, the awareness of elevated environmental, health, and toxicological significance of PFAS has spurred initiatives to collectively address PFAS as a single

chemical class in environmental regulations [4]. However, “PFAS” includes thousands of different molecular structures that vary in the number of C-F bonds, functional groups, and the presence of heteroatoms. The majority of PFAS are anionic, however, non-ionic and zwitterionic PFAS also exist [2].

Removing PFAS from water is a challenging task due to their low reactivity associated with strong C-F bonds in their molecular structure, their generally high hydrophilicity and most often negative charge. In addition, PFAS concentrations that commonly need to be removed from waters are in the ng/L to  $\mu\text{g/L}$  range. Thereby they need to be removed from a matrix containing environmental moieties such as dissolved organic carbon (DOC) occurring in the mg/L range, which further challenges PFAS removal [5]. A predominant water treatment technology for removing PFAS involves fixed-bed adsorption. The most

\* Corresponding authors.

E-mail addresses: [navid.saeidi@ufz.de](mailto:navid.saeidi@ufz.de) (N. Saeidi), [gabriel.sigmund@wur.nl](mailto:gabriel.sigmund@wur.nl) (G. Sigmund).

<https://doi.org/10.1016/j.cej.2024.155456>

Received 29 May 2024; Received in revised form 11 August 2024; Accepted 2 September 2024

Available online 3 September 2024

1385-8947/© 2024 The Author(s). Published by Elsevier B.V. This is an open access article under the CC BY license (<http://creativecommons.org/licenses/by/4.0/>).

commonly used adsorbent material is activated carbon (AC) [5,6]. Adsorption affinity of different PFAS at environmentally relevant concentrations on the same AC can vary up to four orders of magnitude depending on the different molecular properties of the PFAS molecules [7,8]. The number of PFAS that are found in the environment is rising, increasing from approximately 4,700 identified substances documented by OECD in 2017 [9] to over 12,000 documented by US EPA in 2023 [10,11]. Thus, there is a crucial need to broaden our understanding of PFAS adsorption to different adsorbent materials. Similarly, when comparing different carbon materials, the adsorption affinities ( $K_d$ ) for a given PFAS at environmentally relevant concentrations (ng/L to  $\mu\text{g/L}$ ) can also vary by up to four orders of magnitude [7,12–14]. This significant variability is attributed to distinct differences in the adsorbents pore size distributions and surface chemistries. For instance, micropores can cause steric effects to retain PFAS molecules and partially positively charged adsorbent surfaces can provide electrostatic adsorption sites. Adsorption interactions driven by the surface chemistry of adsorbents can be characterized by point of zero charge (PZC), anion and cation exchange capacity (AEC and CEC), and the presence of acidic functional groups (e.g., carboxylic groups) to depict the state of surface charge at a specific pH value [12,15,16]. For carbon materials, additionally the H/C elemental ratio can be used as a measure of aromaticity [17–19]; and other heteroatom/C ratios, such as O/C or O+N/C, can be used as measures of surface polarity [18,20].

In addition to conventional AC and biochar (BC), novel adsorbents including ion exchange resins [21], metal organic frameworks (MOFs) [22], modified inorganic minerals [23], polyaniline-based adsorbents [24], and cyclodextrins [21,25] have also been developed to enhance adsorption of PFAS. To date, a fair and comprehensive assessment of the adsorption performance of PFAS across these diverse adsorbents has not been conducted under comparable experimental conditions. The maximum adsorption capacity ( $q_m$ ), a significant parameter for contaminants in the mg/L range or higher, has previously been employed for such an assessment for some of these adsorbent types, including AC and MOFs [26,27]. However, when dealing with PFAS at trace levels ( $\mu\text{g/L}$  range or below), the adsorption affinity based on  $K_d$  (adsorption coefficient) calculated at a specific environmentally relevant concentration is a more meaningful parameter, as  $q_m$  is often far from being reached [28].

The objective of this study is to contribute to the future targeted development of tailored adsorbents and predictive tools for PFAS adsorption by: i) presenting over 500 individual  $K_d$  values calculated at an equilibrium concentration ( $C_e$ ) of  $1 \pm 0.3 \mu\text{g/L}$  from literature, encompassing the adsorption of 44 different PFAS (41 anionic and 3 zwitterionic) on AC and BC (183), cyclodextrins (235), polymer-based adsorbents and resins (56), and inorganic adsorbents and MOFs (37) under comparable experimental conditions (type of water, pH, and initial concentration of PFAS); ii) identifying and discussing drivers and key parameters for PFAS adsorption for structure-based PFAS sub groups as well as sorbent types via analyses of molecular properties aided by computational methods including homologous series and Butina clustering algorithm; and iii) scope and assess the feasibility of developing predictive models based on existing data and parameters reported in literature. Our insights will advance the toolbox of researchers and practitioners to predict sorbent performance under various conditions, reducing the need for extensive testing and assisting a targeted selection of sorbent for PFAS.

## 2. Methods

All information, such as name and molecular properties of the PFAS, adsorption parameters, experimental condition (pH and type of water), specific surface areas and surface chemical properties of the adsorbents, was gained from literature and is comprehensively shown in the CSV files provided as [Supplementary Information](#) (SI), referred to as CSV SI files in the text. All data and information, along with their references,

are listed in the provided Excel (.xlsx) file. Additionally, a Word document is provided as [supplementary information](#) (referred to in the text as the word SI file) for further explanation and data illustration.

### 2.1. Data mining from the literature

A manual search spanning the years 2015 to 2023 was conducted on October 2023 by Scopus, Web of Science, and Google Scholar searches. Each search included one keyword for adsorption, one keyword for removal, one keyword for Per- and Polyfluorinated Substances (PFAS), and one keyword for adsorbent. Reviews as well as irrelevant or incomplete experimental articles (papers) were subsequently excluded from the database, yielding a refined list of 145 papers. In the second stage of refinement, papers with irrelevant experimental conditions (e.g., due to their specific water conditions, excessively high PFAS concentrations with equilibrium concentrations range after adsorption ( $C_e$ )  $> 100 \mu\text{g/L}$ , or extreme pH) were excluded from the database. Ultimately, 56 papers were used for the extraction of  $K_d$  values.

Single-point adsorption coefficients  $K_d$  were calculated by either experimental adsorption isotherms data or data from single batch adsorption experiments. For all calculations  $C_e$  range of  $1 \pm 0.3 \mu\text{g/L}$  was selected as precondition for calculating  $K_d$  values to have a fair comparison between  $K_d$  values and to investigate the adsorption parameters at environmentally relevant concentrations. In case of single batch experiments, if  $K_d$  was reported,  $C_e$  was calculated from Eq. 1 to see if it is in our targeted range ( $1 \pm 0.3 \mu\text{g/L}$ ).

$$K_d = \frac{q_e}{C_e} \quad (1)$$

In all equations,  $C_e$  denotes equilibrium concentration of PFAS in water ( $\mu\text{g/L}$ ) and  $q_e$  denotes equilibrium concentration of PFAS on the adsorbent ( $\mu\text{g/kg}$ ). In Eq. 1,  $K_d$  is calculated in L/kg. The units of these parameters differ between studies and were harmonized for data analysis here.

In case of non-linear isotherms reported as Freundlich isotherms (Eq. 2) and in which  $C_e$  range covers  $1 \mu\text{g/L}$  the  $K_d$  values were calculated at  $C_e = 1 \mu\text{g/L}$ . At this specific aqueous concentration  $K_d$  is equal to  $K_F$ .

$$q_e = C_e^n * K_F \quad (2)$$

with  $K_F$  ( $(\mu\text{g/kg})/(\mu\text{g/L})^n$ ) which is the Freundlich constant denoting the adsorption affinity, while  $n$  is the Freundlich exponent (dimensionless).

Some other studies did not report  $K_d$  values directly from single batch experiments. Instead they reported other adsorption parameters from which  $K_d$  values could be calculated. For instance, removal or depletion percentage (Re%) from single batch experiment was reported by some studies. In this case, Eq. (3) was applied for calculating  $C_e$ . If  $C_e$  was in our targeted range, Eq. (4) (for calculation of  $q_e$ ) and Eq. (1) (for calculation of  $K_d$ ) were used.

$$C_e = C_0 - \left( \frac{\text{Re}\%}{100} \times C_0 \right) \quad (3)$$

$$q_e = \frac{V \times (C_0 - C_e)}{m} \quad (4)$$

In Eq. (3),  $C_0$  ( $\mu\text{g/L}$ ) denotes the initial concentration of PFAS in water. In Eq. (4)  $V$  (L) denotes the volume of solution and  $m$  (kg) is the mass of the adsorbent.

All calculated  $K_d$  values can be found in CSV SI files ([Table S2–S5](#)) together with the name and properties of compound, experimental condition (pH and type of water), adsorbent name, and adsorbent properties for each individual calculated value.

### 2.2. Adsorbent classification

The adsorbents were classified into four groups: 1- AC and BC, 2-

Cyclodextrins (cyclodextrin-based adsorbents), 3- Polymer-based adsorbents and resins, and 4- Inorganic adsorbents and MOFs. This grouping was carried out considering similarities in the precursors and preparation/synthesis procedures to gain the respective materials.

### 2.3. PFAS molecular properties

The  $K_d$  values were calculated from adsorption studies of 44 types of PFAS listed in Table S1 in the CSV SI files, including 41 anionic and 3 zwitterionic PFAS based on their pH dependent speciation. The Table S1 shows full name of PFAS, simplified molecular input line entry system (SMILES), abbreviations, C number, F number, C-F bond number, molecular weight, charge state at pH 6–8 (the range of pH of the studies from which  $K_d$  values were extracted), number of aromatic rings, water solubility, type of functional group (sulfonic or carboxylic),  $\log K_{OC}$  (soil organic carbon/water partition coefficient),  $\log P_{OW}$  (octanol/water partition coefficient of neutral species),  $pK_a$  (acid dissociation constant), McGown molar volume, and  $\log D_{ow}$  (pH-dependent octanol–water partitioning) at pH 7.

### 2.4. Structure-based grouping of PFAS

Grouping PFAS, together with sorbent classification (section 2.2) was applied to reduce complexity in the dataset, and support relating  $K_d$  trends to structural properties, as well as developing predictive models. The PFAS compounds were grouped using two structure-based cheminformatics approaches. Grouping Method 1 involved classification of PFAS into homologous series using the OngLai algorithm [29], openly implemented in Python using the RDKit [30]. Homologous series are groups of structurally very similar compounds: they share a common core substructure attached to a polymer chain consisting of different numbers of monomer repeating units. A known repeating unit structure is given to OngLai in SMARTS format as input, and through successive fragmentation steps, is removed to isolate the core fragment used as the common denominator for grouping homologous compounds. Here,  $CF_2$  (represented as '[\*#6](-[#9])(-[#9])' in SMARTS) was the repeating unit used as input for homologous series grouping.

Grouping Method 2 leveraged the Butina clustering algorithm implemented in the clusterama library (<https://github.com/PatWalters/clusterama>) based on the original Butina implementation in the RDKit. Molecules were first converted into RDKit fingerprints, then clustered using a Tanimoto similarity cutoff of 0.7 such that molecules in a cluster have maximum distance of 0.3 from each cluster center.

### 2.5. Predictive Modelling of $K_d$ using Random Forest

To further explore the drivers of PFAS sorption, a random forest regression (RFR) model using the scikit-learn Python library (v1.3.1) [31] was developed to predict  $K_d$  based on sorbent descriptors and PFAS molecular properties for AC and BC. This group of adsorbents was selected because of the relatively high number of data and the quality of available sorbent descriptors that based on expert knowledge could be related to sorption. RFR is an ensemble machine learning method that averages the prediction results of multiple decision trees, each constructed using a bootstrap sample of the training dataset (train-test split: 67 % and 33 %). Given the relatively small size of the dataset RFR was chosen for its interpretability and robustness to avoid overfitting.

Feature engineering to prepare the parameters for model development included: Log transformation of  $K_d$  (L/kg) removal of outliers ( $\log K_d < 3.5$ ); imputation of pH 7 for missing pH values (4 out of 183 data) or pH values cited as “6 to 8” (17 out of 183 data) to reflect adsorbents’ buffering pH; creation of a new feature “delta PZCpH” by calculating the difference between PZC and pH indicating the overall charge state of the adsorbent (negative values correspond to negative surface charge and positive values correspond to positive surface charge); and removal of categorical variables and rows with missing property values. The model

was tuned by varying the numbers of trees ( $n_{estimators}$ ) and different combinations of features. The coefficient of determination ( $R^2$ ), Mean Absolute Error (MAE), Root Mean Squared Error (RMSE), and Accuracy (Mean Absolute Percentage Error subtracted from 100) were used for evaluation to select the final model.

## 3. Results and discussion

### 3.1. Comparing adsorption affinities across PFAS chain length and adsorbent types

The length of the fluorinated carbon chain significantly affects their molecular properties and adsorption affinities [32,33]. While the number of carbon atoms indicates overall PFAS size, compounds like perfluorocarboxylic acids and perfluorosulfonic acids with the same carbon counts exhibit different adsorption behaviors that can be related to their different number of C-F bonds. Therefore, comparing the adsorption of different PFAS based on the number of C-F bonds has become widely accepted as preferable over total carbon chain length [14,34]. Hence, we compare adsorption of different PFAS based on the number of C-F bonds.

When evaluating the best performing adsorbents, AC and BC consistently outperformed others in terms of  $K_d$  at  $C_e = 1 \pm 0.3 \mu\text{g/L}$ , with  $K_d$  values sometimes exceeding  $10^7 \text{ L/kg}$  (Fig. 1). Subsequently to the best performing AC and BC group, the adsorption affinity using this criterion followed cyclodextrins, polymer-based adsorbents and resins, and inorganic adsorbents and MOFs, with  $K_d < 10^7 \text{ L/kg}$ . Fig. 1 summarizes the  $K_d$  of all 44 PFAS as function of number of C-F bonds for all four groups of adsorbents. To compare  $K_d$  values across the scattering data, we averaged  $K_d$  values for each adsorbent group (represented by dashed colored lines in Fig. 1). For PFAS with more than 7 C-F bonds, AC and BC had  $K_d$  values  $> 10^7 \text{ L/kg}$ , whereas other adsorbents were below this threshold. The trend held for C-F bonds  $\geq 4$ , though with smaller differences. For C-F bonds  $< 4$ , cyclodextrins, polymer-based adsorbents and resins outperformed AC and BC. This trend also holds when

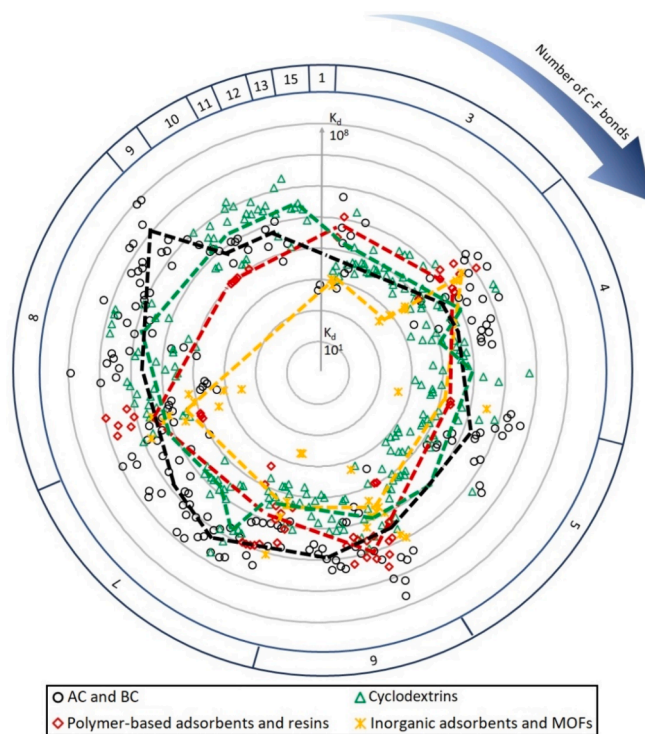


Fig. 1. Adsorption of PFAS as  $K_d$  (L/kg) to 4 groups of adsorbents (see legend for symbols and colors) versus number of C-F bonds. The dashed colored Lines serve as visual guides, indicating the average  $K_d$  values exhibited by each adsorbent group.

considering the highest reported  $K_d$  values for a given C-F bond number and sorbent.

The highest  $K_d$  values, reaching up to  $10^8$  L/kg, were reported for the adsorption of PFOS (number of C-F bonds 8) on thermally surface-modified AC materials treated with reducing atmospheres  $H_2$  [7] and Ammonia [20], and adsorption of PFNA and 6:2 FTS on a commercial AC (Filtrisorb 400) [24]. Overall, the largest variation in adsorption was observed with AC and BC, whereas the most consistent performance was observed for cyclodextrins. Thereby, the more consistent performance of cyclodextrins over AC and BC may be attributed to the diverse range of adsorbent properties of the latter materials, including the range in surface chemistries and the variation in pore size distribution across the AC and BC investigated [14,17]. Combining AC with e.g. cyclodextrins or anion exchange resins for the efficient removal of both short- and long-chain PFAS in a serial two-adsorber setup may be a viable and necessary strategy to address the challenge of remediating water contaminated with various types of PFAS.

### 3.2. Molecular properties driving PFAS adsorption

The  $K_d$  of PFAS correlated positively with hydrophobicity (number of

C-F bonds and  $\log D_{ow}$  at pH 7) and steric properties (molar volume) for AC and BC, as well as cyclodextrins (Fig. 2). No clear correlation between  $K_d$  and the molecular properties of PFAS was observed for polymer-based adsorbents and resins as well as inorganic adsorbents and MOFs (Fig. 2). The molecular properties of PFAS considered in Fig. 2 offer insights into the general adsorption behavior of PFAS on AC and BC, as well as cyclodextrins. However, the  $K_d$  of specific PFAS with comparable hydrophobicity and steric properties at specific adsorbents can vary widely.

Moreover, PFAS with similar number of C-F bonds, molar volume, and  $\log D_{ow}$  may exhibit diverse molecular structures, influencing their adsorption behavior. To further elucidate the relationship between these properties and  $K_d$ , the PFAS structures were grouped into 6 homologous series using the OngLai algorithm. 29 PFAS molecules were located in clusters containing more than one molecule. The groups were generally consistent when using the Butina algorithm, which generated 6 clusters containing more than one molecule per cluster (and 8 others with only 1 molecule per cluster). Compared to the homologous series, the 6 clusters had some minor differences in each group (see Fig. 1S and 2S in the word SI file).

Fig. 3 shows the  $K_d$  distribution for the 6 groups based on the

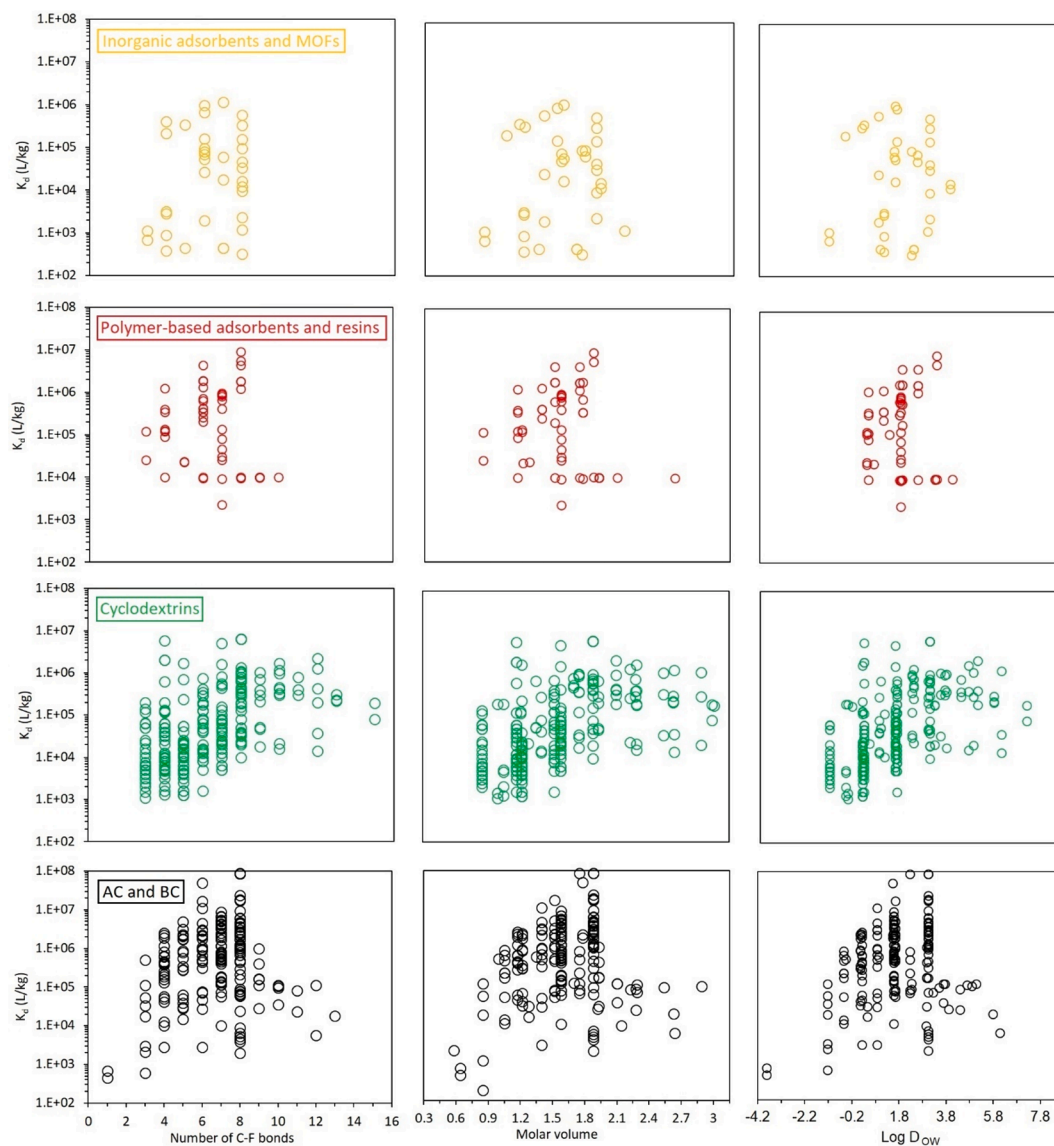


Fig. 2. Adsorption of PFAS as  $K_d$  (L/kg) to the various groups of adsorbents versus molecular properties of the PFAS. For molecular properties, see the CSV file in the SI.

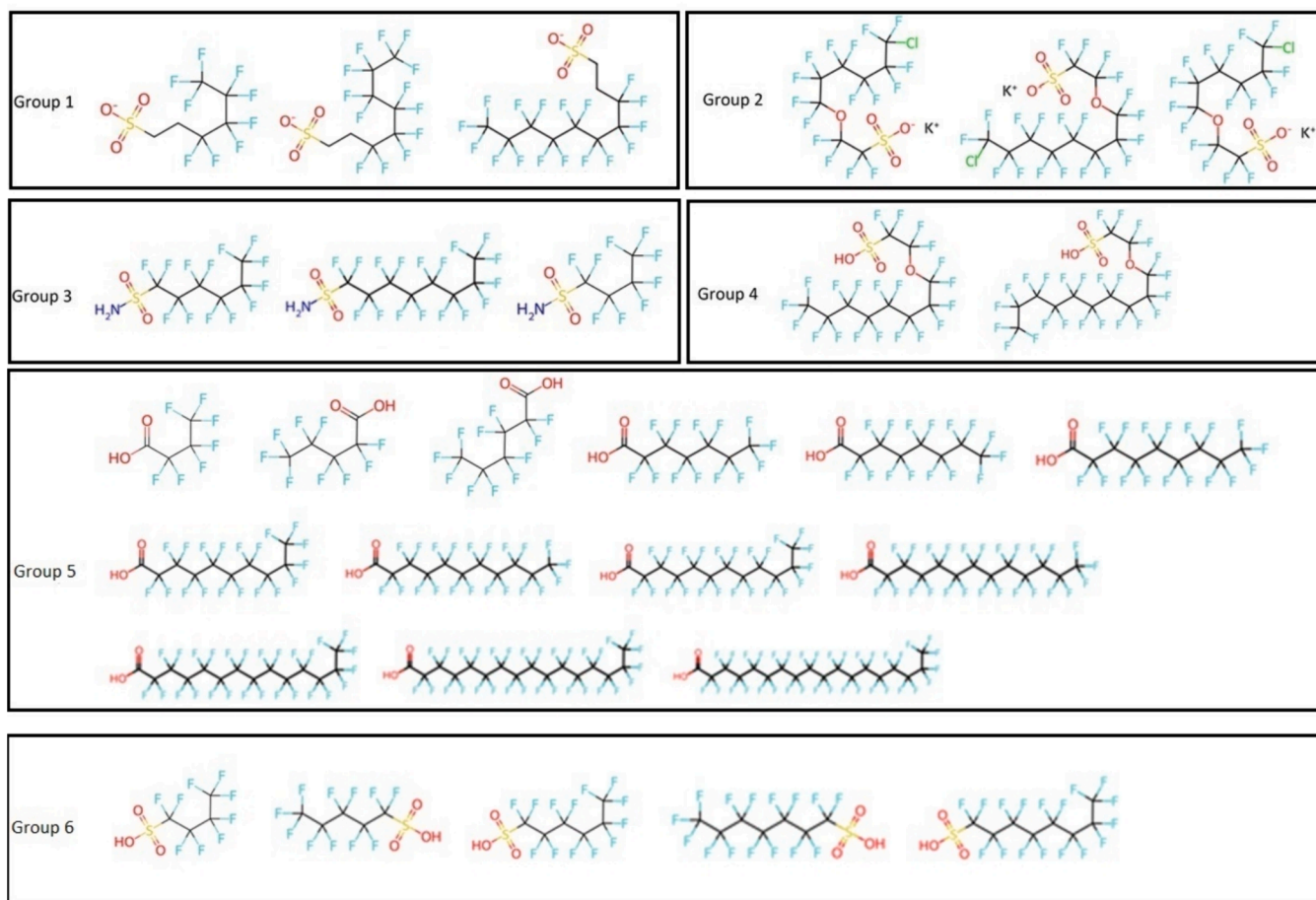
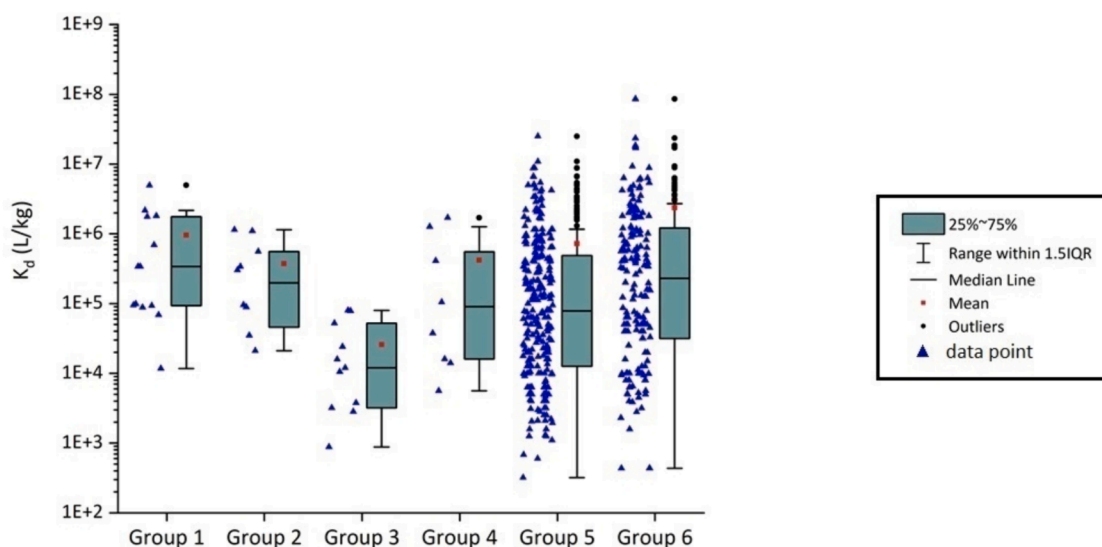


Fig. 3. Deviations in  $K_d$  (L/kg) values within 6 groups of PFAS on all 4 groups of adsorbent materials clustered by homologous series algorithm. Group 1:  $n = 13$ , group 2:  $n = 9$ , group 3:  $n = 11$ , group 4:  $n = 8$ , group 5:  $n = 270$ , and group 6:  $n = 177$ .  $n$  denotes the number of data points.

homologous series approach indicating that the structure-based grouping is reflected in the adsorption behavior. Thus, molecular properties, including the presence of non-fluorinated carbon atoms in the backbone, the type of atom bonded to the non-fluorinated carbon atom, the charge state, and the type of head functional group, influence the adsorption of PFAS. Examining the median line in the scatter plot of

Fig. 3, groups 1 (1 non-fluorinated C atom) and 6 (fully fluorinated C atoms), both featuring a sulfonic acid head group, possessed the highest  $K_d$  across all adsorbent types. It is followed by group 2 (3 non-fluorinated C atoms, sulfonic acid head group, an oxygen atom in the carbon backbone, and a chlorine in the tail), group 4 (2 non-fluorinated C atoms, sulfonic acid head group, and an oxygen atom in the carbon

backbone), group 5 (fully fluorinated C atoms and carboxylic acid head group), and group 3 (fully fluorinated C atoms with sulfonamide head group). Considering only functional head groups, the groups containing PFAS molecules with sulfonic acid head group showed higher  $K_d$  than the molecules with carboxylic acid head group, based on the median  $K_d$ . The PFAS molecules with sulfonamide head group showed the lowest median  $K_d$ .

Fig. 3S in the word SI file provides a visual representation of the data points presented in the scatter plot of Fig. 3 for each adsorbent group. Perfluorocarboxylic acids (Group 5) and perfluorosulfonic acids (Group 6) are the most extensively researched PFAS in adsorption studies. The higher availability of sorption data for these two groups of PFAS allowed for a more in-depth analysis for the two most studied adsorbents (Fig. 4).

Group 6 exhibits higher adsorption affinities compared to group 5 on AC and BC as well as cyclodextrin. The AC and BC had overall higher adsorption affinities compared to cyclodextrin, but cyclodextrins exhibit a more stable performance, as evidenced by the lower scatter observed in Fig. 4. This is likely due to the large variety of material properties in the AC and BC group [14,17] compared to the more consistent properties across cyclodextrins.

### 3.3. Adsorbent properties driving PFAS adsorption

#### I) Relations between AC and BC properties and $K_d$ .

For AC and BC the  $K_d$  for PFAS and specific surface area (SSA) are interrelated (Fig. 5a) with a higher SSA being favorable for stronger adsorption. High SSA is a widely accepted adsorbent descriptor often linked to adsorption performance, which can be related to available adsorption sites and micro- and mesopore spaces [35]. However, additional factors that are SSA independent also contributed to the variation in  $K_d$ , such as surface functional groups and surface charge. Specifically, the net charge on the adsorbents at a given pH, assessed through determination of the PZC, correlates with  $K_d$  values even for SSA normalized  $K_d$  values. A higher PZC (i.e., less negative surface charge) generally results in higher  $K_d$  (Fig. 5b). Given that the experiments were conducted at a pH range of 6–8 (see Table S2–S5 in the CSV SI files), the net charge on the AC and BC is positive when  $PZC > 7$  and negative when  $PZC < 7$ . The PFAS considered in Fig. 5 are all anionic under the

experimental conditions, indicating a significant positive role for electrostatic attraction in the adsorption process whenever  $pH < PZC$  (adsorbent surface net charge is positive) and negative role for electrostatic repulsion whenever  $pH > PZC$  (adsorbent surface net charge is negative). This explains the substantial variation in the adsorption of PFOS, PFOA, PFBS, and PFBA on AC and BC (Fig. 5d). A consistent trend for these compounds persisted across the changes in PZC and adsorbent surface net charge, with adsorption strength following the order: PFOS > PFOA > PFBS > PFBA. This order is consistent with the hydrophobicity ( $\log D_{OW}$  at pH 7 are  $3.05 > 1.58 > 0.25 > -1.22$ , details in Table S1 in the CSV SI files) and the molar volume ( $1.88 > 1.58 > 1.17 > 0.85 \text{ cm}^3 \text{ mol}^{-1} / 100$ , details in Table S1 in the CSV SI files) of these compounds.

Thus, alongside electrostatic interactions, hydrophobic and steric effects significantly influence the adsorption of these PFAS on AC and BC.

The complex adsorption behavior of PFAS is influenced not only by the molecular properties of PFAS but also by the properties of AC and BC. The charge distribution and surface chemistry of carbon adsorbents play significant roles in adsorption of PFAS [7]. These can be characterized by: i) PZC, anion and cation exchange capacity (AEC and CEC), and the content of acidic functional groups (e.g., carboxylic groups) to describe the surface charge state at a specific pH value [12,15,16]; ii) H/C elemental ratio as a measure of aromaticity [17,18]; and iii) other heteroatom/C ratios such as O/C or O+N/C as measures of surface polarity [18,20]. In this study, we correlated the adsorption behavior of PFAS with PZC of AC and BC. An assessment using other aforementioned adsorbent's charge state and surface chemistry properties is currently unfeasible due to a lack of available data. Future research should focus on providing a comprehensive evaluation of adsorbents' charge distribution and surface chemistry when studying the adsorption of PFAS on AC and BC.

#### II) Relations between cyclodextrin properties and $K_d$ .

For cyclodextrins, no clear correlation was found between  $K_d$  and SSA as well as N wt%, and O% (Fig. 4S in the word SI file). An increase in H/C ratio and a related decrease in aromaticity for the adsorbent appeared to be favorable for a stronger adsorption of some PFAS on cyclodextrins (Fig. 6 a and b). The absence of available data of both qualitative and quantitative properties, such as PZC (for assessing adsorbent net charge) and the density of charge compensating sites for anions (like anion exchange capacity), respectively, hinders a more in-depth assessment. No link was identified between  $K_d$  and available adsorbent properties for polymer-based adsorbents and resins as well as inorganic adsorbents and MOFs.

### 3.4. Environmental sorption parameter ( $K_{OC}$ ) is not well translatable to adsorption coefficients in engineered systems

The distribution coefficient between soil organic carbon and water ( $K_{OC}$ ) is widely used in environmental fate assessment and regulation [36]. However, as we show here, regardless of adsorbent,  $K_{OC}$  is not necessarily a good direct predictor for PFAS behavior in engineered adsorbent systems.  $K_{OC}$  can to a small extent predict relative preference in  $K_d$  of PFAS on AC and BC, and cyclodextrins (Fig. 7a and b, respectively). However,  $K_{OC}$  deviates from  $K_d$  up to 5 (AC and BC) and 4 (cyclodextrins) orders of magnitude. For the other adsorbent types considered, the relationship is even weaker (Fig. 5S in the word SI file). The high variability in AC and BC adsorption of PFAS with similar  $K_{OC}$  translates for a typical adsorber unit into anticipated breakthrough times (calculated by Eq. 1S in the word SI file) from less than a day to hundreds of years (10,000 months reached), depending on the specific AC and BC and PFAS molecular properties (Fig. 7c).

This further emphasizes the need for a better understanding and control of adsorption processes for PFAS on AC and BC, especially for those considered to be very mobile in the environment. For cyclodextrins the calculated breakthrough time is always  $< 1,000$  months (Fig. 7d).

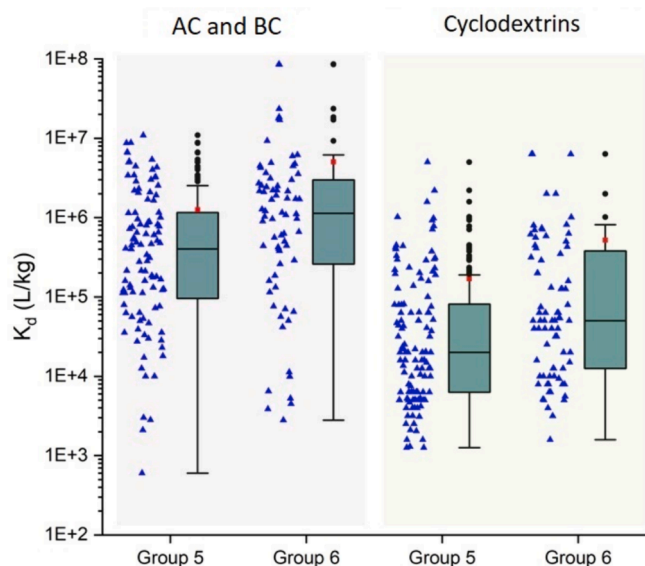
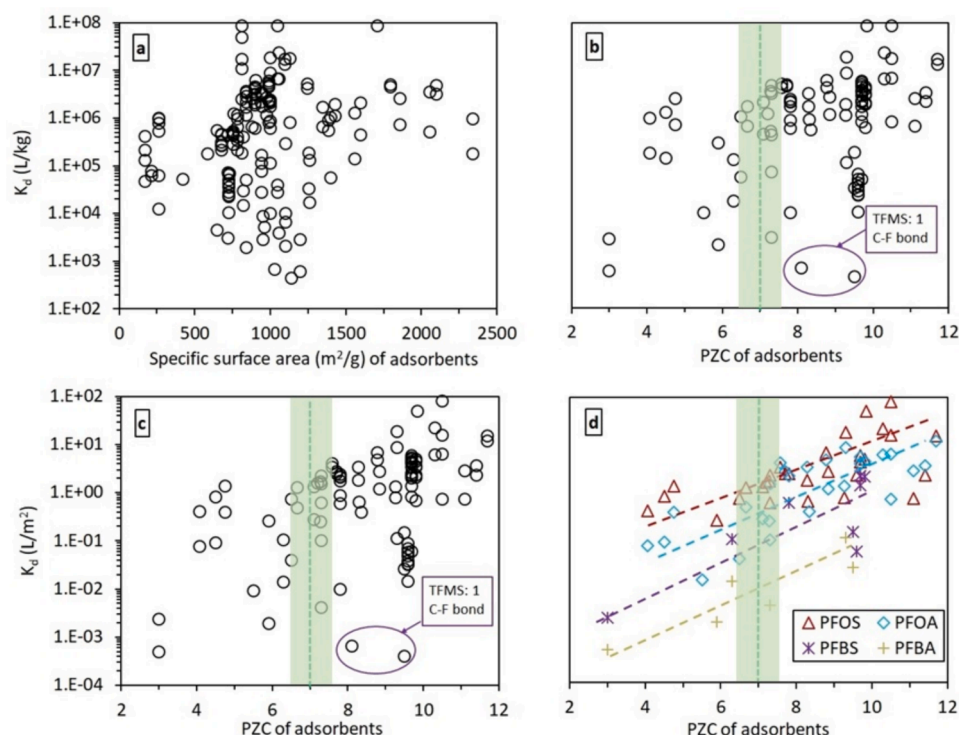
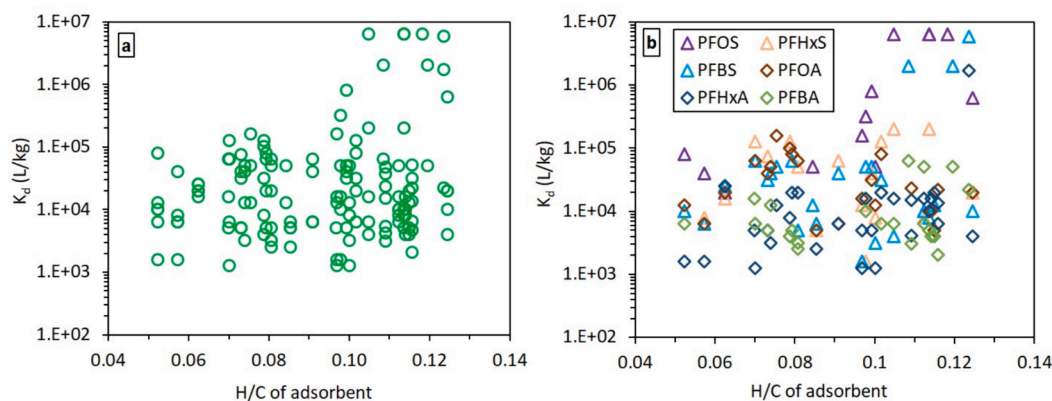


Fig. 4. Comparison of PFAS group 5 and group 6 on two types of adsorbents (AC and BC and cyclodextrins), selected based on their extensive experimental data and frequent use in PFAS removal applications. Group 5: AC and BC  $n = 104$ ; cyclodextrins  $n = 122$ , group 6: AC and BC  $n = 69$ ; cyclodextrins  $n = 79$ .  $n$  denotes the number of data points.



**Fig. 5.**  $K_d$  of PFAS to AC and BC adsorbents versus their SSA (a).  $K_d$  of PFAS versus PZC of the adsorbents (b).  $K_d$  of PFAS normalized to SSA of the adsorbents versus PZC of the adsorbents (c).  $K_d$  of Perfluorooctanesulfonic acid (PFOS), perfluorooctanoic acid (PFOA), perfluorobutanesulfonic acid (PFBS), and perfluorobutanoic acid (PFBA) normalized to SSA of the adsorbents against PZC of the adsorbents (d). TFMS refers to trifluoromethanesulfonic acid. The green-highlighted areas indicate the pH (of the experiments) at which the net charge state of the adsorbents shifts from negative to positive by increasing PZC towards more acidic pH. (For interpretation of the references to colour in this figure legend, the reader is referred to the web version of this article.)



**Fig. 6.**  $K_d$  in adsorption of PFAS against H/C of cyclodextrins (a).  $K_d$  in adsorption of 3 perfluorosulfonic acids and 3 perfluorocarboxylic acids against H/C of the adsorbent (b). PFHxS refers to Perfluorohexanesulfonic acid and PFHxA refers to Perfluorohexanoic acid. See Table S1 in the CSV SI files for detailed information on the PFAS.

### 3.5. Predicting adsorption to AC and BC using sorbent and molecular properties

Based on the above discussion, AC and BC was the most promising adsorbent group to develop a Random Forest Regressor based predictive model that can be sufficiently well parameterized (e.g., charge related parameters were missing for cyclodextrin). The target variable was defined as  $\log K_d$  (original units: L/kg), with outliers ( $\log K_d < 3.5$ ) removed to obtain a near-normal distribution in the target data. Of all the parameters used, surface area ( $\text{m}^2/\text{g}$ ) was the most important, which agrees with the positive correlation between  $K_d$  and SSA (Fig. 5a). Additional input parameters were the difference between PZC and pH ( $\Delta \text{PZCpH}$ ) as a proxy for the adsorbents charge state,  $\log D_{ow}$  (at pH

7), the McGowan molar volume ( $\text{cm}^3 \text{mol}^{-1}/1000$ ),  $\log K_{OC}$  from soil sorption literature, and number of C-F bonds, ranked in that decreasing order based on their feature importance scores. When evaluated on the test set an accuracy of 92.89 % could be reached, which means that a given prediction is only erroneous by 7.11 % on average. For reproducibility and more details, the code for model development, training, and tuning is available as a Jupyter notebook: <https://doi.org/10.5281/zenodo.13258371>.

Fig. 8 shows the comparison between predicted with observed values of  $\log K_d$  of the test set. Despite the small training dataset ( $n = 60$  points), the RFR model achieved a high accuracy, implying a satisfactory performance of RFR for the present task. However, the relatively low  $R^2$  value indicates that the variance of the target variable  $\log K_d$  is not

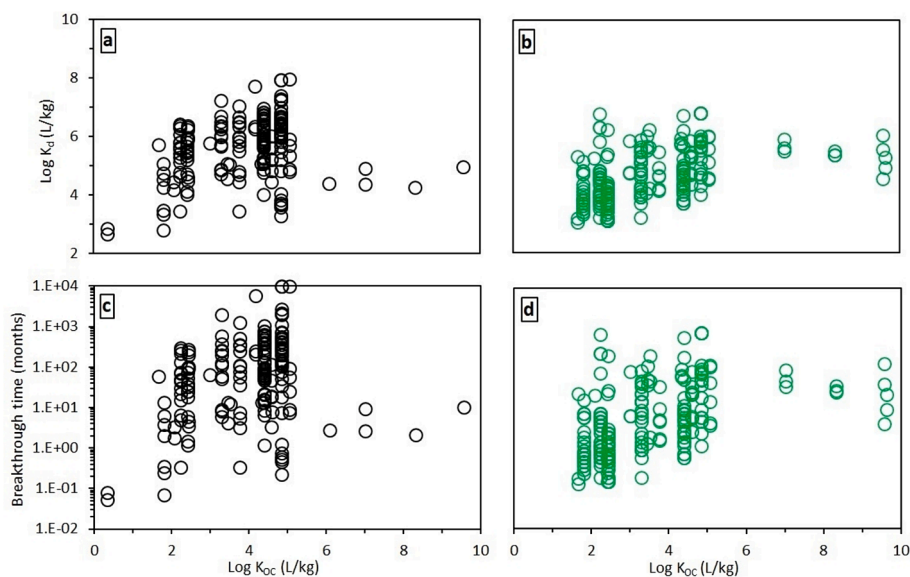


**Fig. 7.** Correlation between  $K_d$  in adsorption of PFAS on AC and BC (a) and cyclodextrins (b) and  $K_{OC}$ . Correlation between  $K_d$  in adsorption of PFAS on AC and BC (c) and cyclodextrins (d) and breakthrough time. Breakthrough time was calculated for a hypothetical adsorbent unit (calculated by Eq. 1S in the SI with approximated  $m_{solid}/V_{void} = 0.67$  kg/L and water residence time ( $t_w$ ) = 15 min).

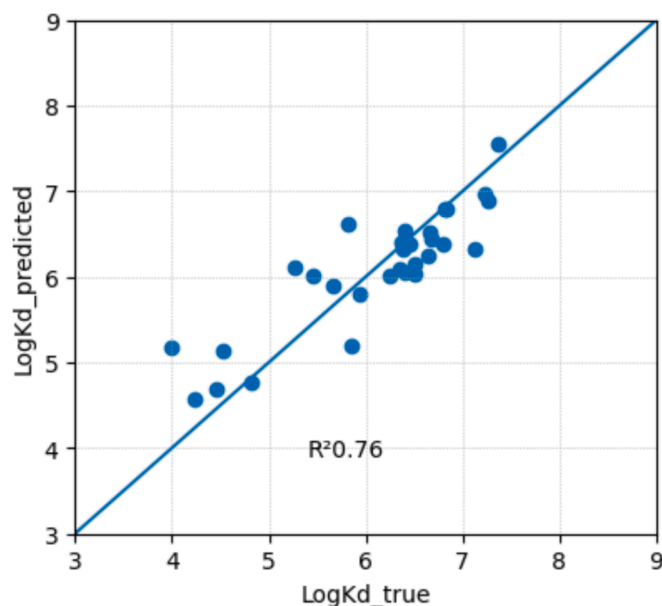


**Fig. 8.** Scatter plot of test set values showing the predicted  $K_d$  ( $\text{Log } K_d_{\text{predicted}}$ ) using the Random Forest Regressor and true values which are observed values obtained from literature ( $\text{Log } K_d_{\text{true}}$ ). Blue line represents 1:1. Original units of  $K_d$  are L/kg,  $n = 60$  datapoints used in training set. RMSE=0.45; MAE=0.35. (For interpretation of the references to colour in this figure legend, the reader is referred to the web version of this article.)

sufficiently captured by the model, which could be due to (i) insufficient features or (ii) data imbalance. Feature engineering to address (i) did not yield significantly better results (see Jupyter notebook). Further, the limited availability of datapoints for some specific combinations is inherent to this study which is based on literature mining, that is for example biased towards some PFAS molecules over others. Thus, we see the clear need for experimentally obtaining further  $K_d$  values for a broader range of PFAS-adsorbent combinations. Hyperparameter tuning by increasing the number of estimators up to 20,000 gave an insignificant improvement in  $R^2$  (increase by approximately 0.001), at the

expense of longer training time and was thus not deemed useful. More advanced hyperparameter tuning via grid search or random search may improve  $R^2$  and could be explored in future studies.

Additionally, more structure-based or molecular features may be added, albeit with caution to avoid the risk of overfitting. Overall, the here introduced model among the first to explore this possibility, serves as a proof-of-concept that  $K_d$  can be predicted using RFR and parameters reported in AC and BC literature, demonstrating that such models are conceptually feasible. However, as stated in [37], creating such models requires overcoming existing data limitations in order to produce more robust and reliable predictions. Generally, across all adsorbent types, a more consistent quantification of sorbent charge state (PZC and/or anion exchange capacity at a given pH) could help make future models more reliable and feasible.

#### 4. Conclusions

When dealing with PFAS with low mobilities and higher hydrophobicity (long-chain PFAS) adsorbents from the AC and BC group lead to a very strong adsorption with  $K_d$  values up to  $10^8$  L/kg and breakthrough time of up to 10,000 months, while  $K_d$  is always  $< 10^7$  L/kg across all other adsorbent types investigated in this study. Information on PZC can aid the selection of suitable AC and BC adsorbents. In future more quantitative surface charge descriptors such as anion exchange capacity that is not available today could be more effective for prediction and exceed the value of PZC in assessing a sorbents suitability. Cyclodextrins were the second-best suitable adsorbents. However, textural and surface chemical properties alone did not allow to reliably predict adsorption performance for PFAS. The aromaticity proxy (H/C ratio), although the best available descriptor, remained a poor indicator.

Hydrophobicity (evaluated by the number of C-F bonds and  $\log D_{ow}$  at pH 7) and steric properties (assessed by molar volume) of PFAS are positively linked to sorption on AC and BC, as well as cyclodextrins. Nevertheless, significant variations were observed in  $K_d$  values for PFAS with similar hydrophobicity and steric properties. In addition, we found that  $K_{OC}$  is not necessarily a good direct predictor for PFAS behavior in engineered adsorbent systems. No correlation between  $K_d$  and PFAS molecular properties was found for polymer-based adsorbents and resins, inorganic adsorbents and MOFs.

The assessment by computational studies revealed that apart from

molecular properties related to hydrophobicity and steric effects, other factors such as the type of head group, number of non-fluorinated carbon atoms, presence of oxygenated carbon in the backbone, and chlorinated carbon atoms at the tail of PFAS can influence their adsorption behavior. Further, we showed that developing Random Forest Regressor based predictive models using available PFAS descriptors and AC and BC descriptors is feasible. Future model development could profit from a wider use of surface charge related parameterization of adsorbents across all adsorbent types when dealing with charged substances, as most PFAS are charged at environmental pH. To maximize the accessibility and usability of our data, we adhered to the FAIR data principles and provided the raw data including PFAS molecular properties,  $K_d$  values, and respective adsorbent properties (CSV SI files).

### CRedit authorship contribution statement

**Navid Saeidi:** Writing – review & editing, Writing – original draft, Visualization, Formal analysis, Data curation. **Adelene Lai:** Writing – review & editing, Visualization, Validation, Formal analysis. **Falk Harnisch:** Writing – review & editing. **Gabriel Sigmund:** Writing – review & editing, Writing – original draft, Visualization, Formal analysis, Data curation, Conceptualization.

### Declaration of competing interest

The authors declare that they have no known competing financial interests or personal relationships that could have appeared to influence the work reported in this paper.

### Data availability

All data and code used are made available

### Appendix A. Supplementary data

Supplementary data to this article can be found online at <https://doi.org/10.1016/j.cej.2024.155456>.

### References

- R.C. Buck, J. Franklin, U. Berger, J.M. Conder, I.T. Cousins, P. de Voogt, A. Jensen, K. Kannan, S.A. Mabury, S.P. van Leeuwen, Perfluoroalkyl and polyfluoroalkyl substances in the environment: Terminology, classification, and origins, *Integr. Environ. Assess. Manag.* 7 (4) (2011) 513–541, <https://doi.org/10.1002/ieam.258>.
- Y. Zhang, Y. Zhou, R. Dong, N. Song, M. Hong, J. Li, J. Yu, D. Kong, Emerging and legacy per- and polyfluoroalkyl substances (PFAS) in fluorochemical wastewater along full-scale treatment processes: Source, fate, and ecological risk, *J. Hazard. Mater.* 465 (2024) 133270, <https://doi.org/10.1016/j.jhazmat.2023.133270>.
- N. Hamid, M. Junaid, R. Manzoor, M. Sultan, O.M. Chuan, J. Wang, An integrated assessment of ecological and human health risks of per- and polyfluoroalkyl substances through toxicity prediction approaches, *Sci. Total Environ.* 905 (2023) 167213, <https://doi.org/10.1016/j.scitotenv.2023.167213>.
- I.T. Cousins, J.C. DeWitt, J. Glüge, G. Goldenman, D. Herzke, R. Lohmann, C.A. Ng, M. Scheringer, Z. Wang, The high persistence of PFAS is sufficient for their management as a chemical class, *Environ. Sci. Processes Impacts* 22 (12) (2020) 2307–2312, <https://doi.org/10.1039/D0EM00355G>.
- E. Gagliano, M. Sgroi, P.P. Falciglia, F.G.A. Vagliasindi, P. Roccaro, Removal of poly- and perfluoroalkyl substances (PFAS) from water by adsorption: Role of PFAS chain length, effect of organic matter and challenges in adsorbent regeneration, *Water Res.* 171 (2020) 115381, <https://doi.org/10.1016/j.watres.2019.115381>.
- H.N. Phong Vo, H.H. Ngo, W. Guo, T.M. Hong Nguyen, J. Li, H. Liang, L. Deng, Z. Chen, T.A. Hang Nguyen, Poly- and perfluoroalkyl substances in water and wastewater: A comprehensive review from sources to remediation, *Journal of Water Process Engineering* 36 (2020) 101393, [10.1016/j.jwpe.2020.101393](https://doi.org/10.1016/j.jwpe.2020.101393).
- N. Saeidi, F.-D. Kopinke, A. Georgi, What is specific in adsorption of perfluoroalkyl acids on carbon materials? *Chemosphere* 273 (2021) 128520 <https://doi.org/10.1016/j.chemosphere.2020.128520>.
- B. Cantoni, A. Turolla, J. Wellnitz, A.S. Ruhl, M. Antonelli, Perfluoroalkyl substances (PFAS) adsorption in drinking water by granular activated carbon: Influence of activated carbon and PFAS characteristics, *Sci. Total Environ.* 795 (2021) 148821, <https://doi.org/10.1016/j.scitotenv.2021.148821>.
- Z. Wang, S25 | OECD PFAS | List of PFAS from the OECD (NORMAN-SLE-S25.0.1.0) . Zenodo. 10.5281/zenodo.2648776 2018.
- US EPA. CompTox Chemicals Dashboard | PFASMASTERChemicals. <https://comptox.epa.gov/dashboard/chemical-lists/PFASMASTER> (accessed 2023–09–17). 2023.
- E.L. Schymanski, J. Zhang, P.A. Thiessen, P. Chirsir, T. Kondic, E.E. Bolton, Per- and Polyfluoroalkyl Substances (PFAS) in PubChem: 7 Million and Growing, *Environ. Sci. Tech.* 57 (44) (2023) 16918–16928, <https://doi.org/10.1021/acs.est.3c04855>.
- Y. Zhi, J. Liu, Adsorption of perfluoroalkyl acids by carbonaceous adsorbents: Effect of carbon surface chemistry, *Environ. Pollut.* 202 (2015) 168–176, <https://doi.org/10.1016/j.envpol.2015.03.019>.
- A. Georgi, J. Bosch, J. Bruns, K. Mackenzie, N. Saeidi, F. Kopinke, *Kolloidale Aktivkohle für die In-situ-Sanierung von PFAS-kontaminierten Grundwasserleitern*, *Altlasten Spektrum* 29 (2020) 232–237.
- K.M. Krahn, G. Cornelissen, G. Castro, H.P.H. Arp, A.G. Asimakopoulos, R. Wolf, R. Holmstad, A.R. Zimmerman, E. Sørmo, Sewage sludge biochars as effective PFAS-sorbents, *J. Hazard. Mater.* 445 (2023) 130449, <https://doi.org/10.1016/j.jhazmat.2022.130449>.
- N. Saeidi, F.-D. Kopinke, A. Georgi, Understanding the effect of carbon surface chemistry on adsorption of perfluorinated alkyl substances, *Chem. Eng. Journal* 381 (2020) 122689, <https://doi.org/10.1016/j.cej.2019.122689>.
- J. Zhou, N. Saeidi, L.Y. Wick, F.-D. Kopinke, A. Georgi, Adsorption of polar and ionic organic compounds on activated carbon: Surface chemistry matters, *Sci. Total Environ.* 794 (2021) 148508, <https://doi.org/10.1016/j.scitotenv.2021.148508>.
- B.M. Aumeier, A. Georgi, N. Saeidi, G. Sigmund, Is sorption technology fit for the removal of persistent and mobile organic contaminants from water? *Sci. Total Environ.* 880 (2023) 163343 <https://doi.org/10.1016/j.scitotenv.2023.163343>.
- G. Sigmund, M. Gharasoo, T. Hüffer, T. Hofmann, Deep Learning Neural Network Approach for Predicting the Sorption of Ionizable and Polar Organic Pollutants to a Wide Range of Carbonaceous Materials, *Environ. Sci. Tech.* 54 (7) (2020) 4583–4591, <https://doi.org/10.1021/acs.est.9b06287>.
- S. Kundu, S. Patel, P. Halder, T. Patel, M. Hedayat Marzbali, B.K. Pramanik, J. Paz-Ferreiro, C.C. de Figueiredo, D. Bergmann, A. Surapaneni, M. Megharaj, K. Shah, Removal of PFASs from biosolids using a semi-pilot scale pyrolysis reactor and the application of biosolids derived biochar for the removal of PFASs from contaminated water, *Environmental Science: Water Research & Technology* 7(3) (2021) 638–649. [10.1039/D0EW00763C](https://doi.org/10.1039/D0EW00763C).
- Y. Zhi, J. Liu, Surface modification of activated carbon for enhanced adsorption of perfluoroalkyl acids from aqueous solutions, *Chemosphere* 144 (2016) 1224–1232, <https://doi.org/10.1016/j.chemosphere.2015.09.097>.
- C. Ching, M.J. Klemes, B. Trang, W.R. Dichtel, D.E. Helbling,  $\beta$ -Cyclodextrin Polymers with Different Cross-Linkers and Ion-Exchange Resins Exhibit Variable Adsorption of Anionic, Zwitterionic, and Nonionic PFASs, *Environmental Science & Technology* 54 (19) (2020) 12693–12702, <https://doi.org/10.1021/acs.est.0c04028>.
- R. Li, S. Alomari, T. Islamoglu, O.K. Farha, S. Fernando, S.M. Thagard, T.M. Holsen, M. Wriedt, Systematic Study on the Removal of Per- and Polyfluoroalkyl Substances from Contaminated Groundwater Using Metal-Organic Frameworks, *Environ. Sci. Tech.* 55 (22) (2021) 15162–15171, <https://doi.org/10.1021/acs.est.1c03974>.
- B. Yan, G. Munoz, S. Sauvé, J. Liu, Molecular mechanisms of per- and polyfluoroalkyl substances on a modified clay: a combined experimental and molecular simulation study, *Water Res.* 184 (2020) 116166, <https://doi.org/10.1016/j.watres.2020.116166>.
- J. He, A. Gomeniuc, Y. Olshansky, J. Hatton, L. Abrell, J.A. Field, J. Chorover, R. Sierra-Alvarez, Enhanced removal of per- and polyfluoroalkyl substances by crosslinked polyaniline polymers, *Chem. Eng. Journal* 446 (2022) 137246, <https://doi.org/10.1016/j.cej.2022.137246>.
- R. Wang, Z.-W. Lin, M.J. Klemes, M. Ateia, B. Trang, J. Wang, C. Ching, D. E. Helbling, W.R. Dichtel, A Tunable Porous  $\beta$ -Cyclodextrin Polymer Platform to Understand and Improve Anionic PFAS Removal, *ACS Central Science* 8 (5) (2022) 663–669, <https://doi.org/10.1021/acscentsci.2c00478>.
- X. Lei, Q. Lian, X. Zhang, T.K. Karsili, W. Holmes, Y. Chen, M.E. Zappi, D.D. Gang, A review of PFAS adsorption from aqueous solutions: Current approaches, engineering applications, challenges, and opportunities, *Environ. Pollut.* 321 (2023) 121138, <https://doi.org/10.1016/j.envpol.2023.121138>.
- P.S. Paultetto, T.J. Bandoz, Activated carbon versus metal-organic frameworks: A review of their PFAS adsorption performance, *J. Hazard. Mater.* 425 (2022) 127810, <https://doi.org/10.1016/j.jhazmat.2021.127810>.
- N. Saeidi, F. Harnisch, V. Presser, F.-D. Kopinke, A. Georgi, Electrosorption of organic compounds: State of the art, challenges, performance, and perspectives, *Chem. Eng. J.* 471 (2023) 144354, <https://doi.org/10.1016/j.cej.2023.144354>.
- A. Lai, J. Schaub, C. Steinbeck, E.L. Schymanski, An algorithm to classify homologous series within compound datasets, *J. Cheminf.* 14 (1) (2022) 85, <https://doi.org/10.1186/s13321-022-00663-y>.
- G. Landrum, RDKit: Open-source cheminformatics., 2023. (Accessed 01.11. 2023).
- F. Pedregosa, G. Varoquaux, A. Gramfort, V. Michel, B. Thirion, O. Grisel, M. Blondel, P. Prettenhofer, R. Weiss, V. Dubourg, J. Vanderplas, A. Passos, D. Cournapeau, M. Brucher, M. Perrot, É. Duchesnay, Scikit-learn: Machine Learning in Python, *J. Mach. Learn. Res.* 12(null) (2011) 2825–2830.
- J.M. Sun, B.C. Kelly, F.A.P.C. Gobas, E.M. Sunderland, A food web bioaccumulation model for the accumulation of per- and polyfluoroalkyl substances (PFAS) in fish: how important is renal elimination? *Environ. Sci. Processes Impacts* 24 (8) (2022) 1152–1164, <https://doi.org/10.1039/D2EM00047D>.
- X. Yun, A.J. Lewis, G. Stevens-King, C.M. Sales, D.E. Spooner, M.J. Kurz, R. Suri, E. R. McKenzie, Bioaccumulation of per- and polyfluoroalkyl substances by

- freshwater benthic macroinvertebrates: Impact of species and sediment organic carbon content, *Sci. Total Environ.* 866 (2023) 161208, <https://doi.org/10.1016/j.scitotenv.2022.161208>.
- [34] S. Ghorbani Gorji, D.W. Hawker, R. Mackie, C.P. Higgins, K. Bowles, Y. Li, S. Kaserzon, Sorption affinity and mechanisms of per-and polyfluoroalkyl substances (PFASs) with commercial sorbents: Implications for passive sampling, *Journal of Hazardous Materials* 457 (2023) 131688. [10.1016/j.jhazmat.2023.131688](https://doi.org/10.1016/j.jhazmat.2023.131688).
- [35] G. Sigmund, T. Hüffer, T. Hofmann, M. Kah, Biochar total surface area and total pore volume determined by N<sub>2</sub> and CO<sub>2</sub> physisorption are strongly influenced by degassing temperature, *Sci. Total Environ.* 580 (2017) 770–775, <https://doi.org/10.1016/j.scitotenv.2016.12.023>.
- [36] G. Sigmund, H.P.H. Arp, B.M. Aumeier, T.D. Bucheli, B. Chefetz, W. Chen, S.T. J. Droge, S. Endo, B.I. Escher, S.E. Hale, T. Hofmann, J. Pignatello, T. Reemtsma, T. C. Schmidt, C.D. Schönsee, M. Scheringer, Sorption and Mobility of Charged Organic Compounds: How to Confront and Overcome Limitations in Their Assessment, *Environ. Sci. Tech.* 56 (8) (2022) 4702–4710, <https://doi.org/10.1021/acs.est.2c00570>.
- [37] S. Back, A. Aspuru-Guzik, M. Ceriotti, G. Gryn'ova, B. Grzybowski, G.H. Gu, J. Hein, K. Hippalgaonkar, R. Hormázabal, Y. Jung, S. Kim, W.Y. Kim, S. M. Moosavi, J. Noh, C. Park, J. Schrier, P. Schwaller, K. Tsuda, T. Vegge, O.A. von Lilienfeld, A. Walsh, Accelerated chemical science with AI, *Digital Discovery* 3 (1) (2024) 23–33, <https://doi.org/10.1039/D3DD00213F>.